ACES Asian Chemical Editorial Society

DOI: 10.1002/asia.201501090

CHEMISTRY AN ASIAN JOURNAL Communication

Supramolecular Chemistry

Temperature-Responsive Chiral $(A)_6B$ Supramolecular Cages Based on Conformational Preferences

Shi-Gui Chen,[a] Zhi-Xiong Zhao,[a] Xiao-Nan Jiang,[a] Lu Wang,[a] Tian-You Zhou,[a] Cheng-Lu Lu,[a] Xin Zhao,*[a] Xi-Kui Jiang,[a] Yuguo Ma,*[b] Ren-Xiao Wang,*[a] and Zhan-Ting Li*[a, c]

Abstract: Two chiral $(A)_6B$-typed supramolecular cages were constructed from hydrogen-bonded C_6-symmetric zinc porphyrin hexamers and chiral C_3-symmetric pyridyl hexadentates with a core of 1,3,5-triphenylbenzene. Circular dichroism and molecular simulations revealed that the symmetry of the supramolecular cages switched from pseudo-C_{3v} to C_3 with the rotational confinement of the biphenyl backbones at low temperatures, which generated conformationally chiral transfer and amplification. This unique phenomenon suggests a new strategy to develop smart materials with high sensitivity and excellent reversibility.

In the past decades, numerous artificial responsive systems[1] have been developed to respond to external triggers, such as pH,[2] temperature,[3] light,[4] redox,[5] mechanical,[6] magnetic,[7] radiation,[8] and biological[8] and chemical analytes.[10] Such smart structures have shown great potential for applications in controlled delivery,[11] chemosensors,[12] and biomedical materials.[13] The probes employed in these systems were usually developed from structural changes,[14] supramolecular interactions[15] or configurational changes.[16] The sensitivity and reversibility of the stimuli-responsiveness highly depend on the energy barrier of the probes. As a ubiquitous phenomenon in nature, the stimuli-responsiveness of biological systems exhibits excellent accuracy, sensitivity and reversibility, which highly rely on conformational preferences of proteins.[17] Utilizing the principle of nature might create more elaborate smart materials. However, conformational preferences have been rarely elucidated in artificial stimuli-responsive systems[18] or employed as probes of stimuli-responsive systems. Therefore, the realization of conformational preferences is of particular importance in the improvement of performance and the development of new artificial stimuli-responsive systems. We herein report a temperature-dependent conformational preference among a kind of chiral seven-component supramolecular cages which displays different conformational chirality at different temperatures.

It has been previously demonstrated that the multivalent self-assembly between hydrogen-bonded C_6-symmetric hexamer $(\mathbf{1})_6$[19,20] and pyridyl hexadentates forms layered supramolecular copolymers, in which the hexadentate linkers with limited-length chains bound hexamer $(\mathbf{1})_6$ from both sides by alternately forming three N-Zn coordination bonds in an induced-fit manner.[21] We envisioned that similar hexadentates **2** (*D* 3.9 nm) and **3** (*D* 4.4 nm) with longer chains might bind hexamer $(\mathbf{1})_6$ (*D* 3.5 nm) from one side via six N-Zn coordination bonds, giving rise to seven-component supramolecular cages $(\mathbf{1})_6$·**2** and $(\mathbf{1})_6$·**3** (Figure 1). The formation of A_6B-type supramolecular cages was firstly ascertained by UV/Vis spectroscopy. Significant red shifts, up to 6.5 and 14 nm in the Soret and Q bands of porphyrin units, respectively, were observed upon the addition of 0.17 equivalent of (*R*)-**2** (1.0 equiv. pyridyl) to **1** (28 μM) (Figure S1, Supporting Information), revealing a strong affinity between hexamer $(\mathbf{1})_6$ and (*R*)-**2** which benefited from the highly cooperative multivalency effect.[21] Well-defined isosbestic points were observed during the titration of **1** with *R*-**2** (Figure S1), suggesting the formation of a single supramolecular entity. The Job's plot confirmed a 6:1 stoichiometry (Figure S2). The nonlinear least-squares fitting of the UV/Vis titration data gave an apparent association constant of $1.7\times10^7\ M^{-1}$ for the complex of the zinc porphyrin of **1** and R-**2**,[22] which was much higher than those of complexes from monotopic zinc porphyrin/nitrogen ligand coordination interactions,[23] indicating multivalent cooperation between hexamers $(\mathbf{1})_6$ and hexadentates (*R*)-**2**. Similar red shifts and isosbestic points were also observed from the UV/Vis titration of **1** with *R*-**3**, which gave an apparent association constant (K_{assoc}) of $2.7\times10^7\ M^{-1}$ for **1** and *R*-**3** (Figure S3). The diffusion coefficients

[a] Dr. S.-G. Chen, Dr. Z.-X. Zhao, Dr. X.-N. Jiang, Dr. L. Wang, Dr. T.-Y. Zhou, C.-L. Lu, Prof. Dr. X. Zhao, Prof. Dr. X.-K. Jiang, Prof. Dr. R.-X. Wang, Prof. Dr. Z.-T. Li
Shanghai Institute of Organic Chemistry
Chinese Academy of Sciences
345 Lingling Lu, Shanghai 200032 (China)
E-mail: xzhao@mail.sioc.ac.cn
wangrx@mail.sioc.ac.cn
ztli@mail.sioc.ac.cn

[b] Prof. Dr. Y. Ma
Beijing National Laboratory for Molecular Sciences
Key Laboratory of Polymer Chemistry and Physics of Ministry of Education
College of Chemistry
Peking University
Beijing 100871 (China)
E-mail: ygma@pku.edu.cn

[c] Prof. Dr. Z.-T. Li
Department of Chemistry
Fudan University
220 Handan Road, Shanghai 200433 (China)

Supporting information for this article is available on the WWW under http://dx.doi.org/10.1002/asia.201501090.

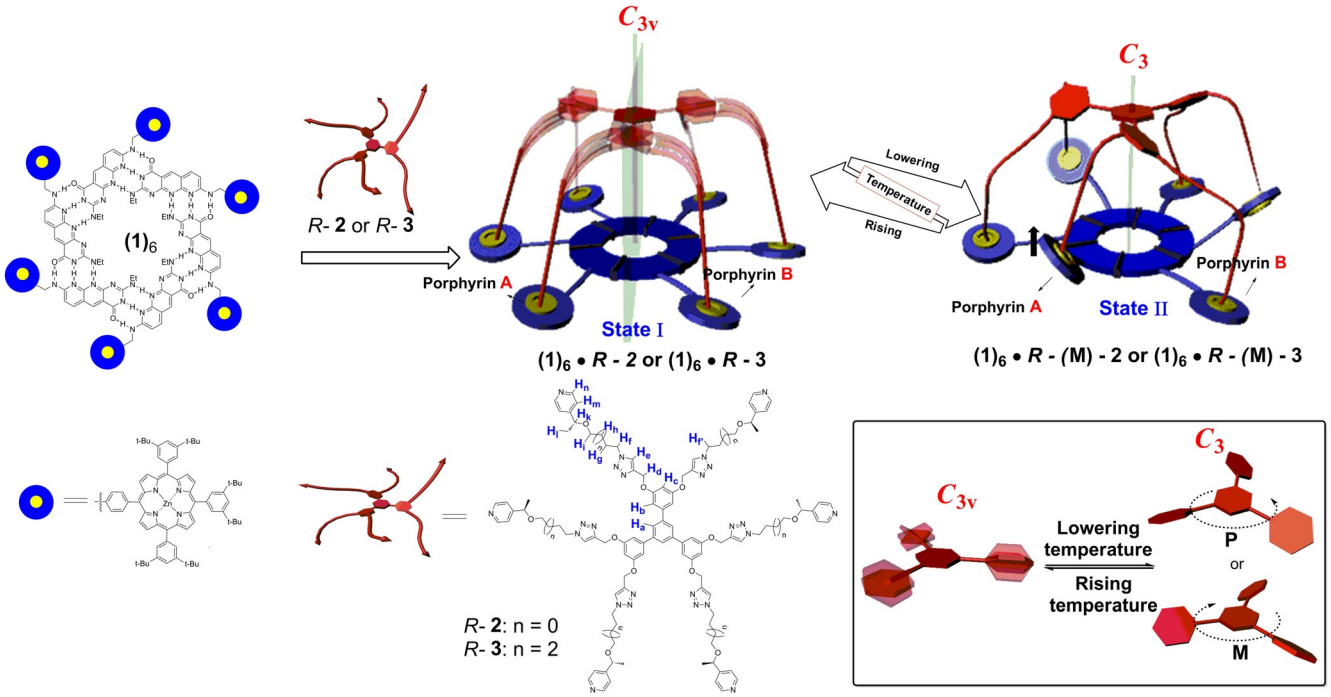

Figure 1. Schematic representation of the formation of $(A)_6B$-typed chiral supramolecular cages that exhibited temperature-dependent conformational preference. The inset at the right bottom shows the possible conformations of 1,3,5-triphenylbenzene at low temperature, which were determined by the chirality of the C_3 molecules and confined at low temperatures.

(D) for **1**, the mixtures of **1**/(*R*)-**2** (1: 0.17), and **1**/(*R*)-**3** (1:0.17) ([1] = 4.8 mM) in $CDCl_3$ were measured by two-dimensional diffusion-ordered NMR (DOSY) experiments to be 6.1×10^{-9}, 5.0×10^{-9}, and 4.9×10^{-9} m^2s^{-1}, respectively. The values of the mixtures were gently but solidly lower than that of **1**, in accordance with the formation of complexes $(\mathbf{1})_6$·(*R*)-**2** or $(\mathbf{1})_6$·(*R*)-**3** of larger sizes, which also indicated little aggregation between the complexes.

The temperature dependence of $(\mathbf{1})_6$·*R*-**2** was first revealed by UV/Vis experiments (Figure S4). The Soret band of the porphyrin units underwent a blue-shift by 1.5 nm with broadening and weakening of the absorption peak upon the increase of the temperature from 20 °C to 50 °C, suggesting an increase of the conformational diversity of the porphyrin units in the complex $(\mathbf{1})_6$·(*R*)-**2**. Reverse changes were observed when the temperature was decreased from 20 °C to −50 °C: the Soret band red-shifted by 1.0 nm, and the peak became sharp and the intensity increased, implying that the thermodynamic motions of the porphyrin units slowed down to form more compact aggregates. With the addition of hexadentate *R*-**2** to hexamer $(\mathbf{1})_6$, the proton resonances of both $(\mathbf{1})_6$ and *R*-**2** became broader and showed significant shifting, in line with the formation of complex $(\mathbf{1})_6$·*R*-**2** (Figure S5). All the proton signals of *R*-**2** shifted upfield, indicating the strong shielding effects by the large aromatic rings of $(\mathbf{1})_6$. All proton signals of the complex became obviously broad when the temperature was lowered (Figure 2). For *R*-**2**, the broadening of H_f resulted in a split of the peak into two peaks at −70 °C, indicating the completion of the transformation from State I to State II (Figure 1).

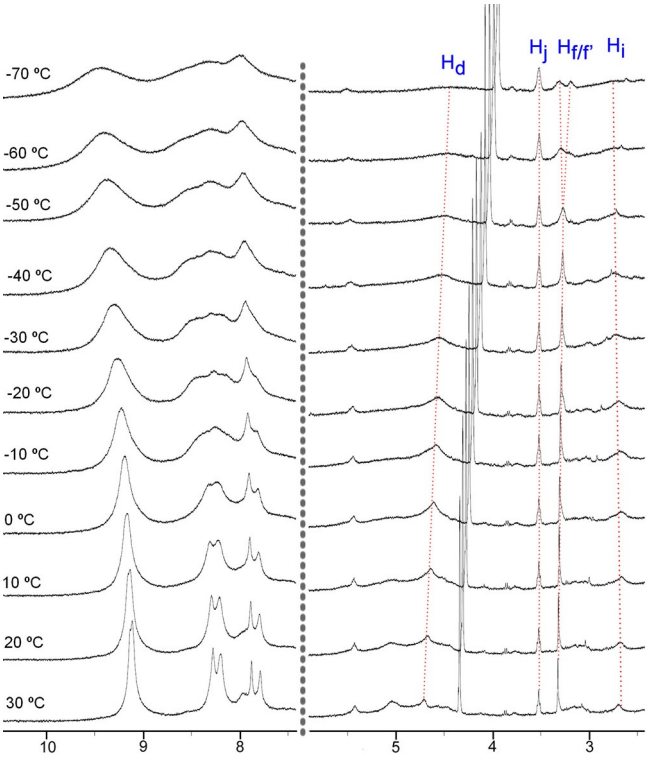

Figure 2. Selected regions of variable-temperature (VT) ^1H NMR spectra (400 MHz) of complex $(\mathbf{1})_6$·*R*-**2** in $[D_8]$toluene/CD_2Cl_2 (9:1), showing the broadening of the signals and the splitting of proton H_f of *R*-**2** into two peaks with the decrease of temperatures. The signals of aromatic protons $H_{a=c,e,m,n}$ were overlapped with that of hexamer $(\mathbf{1})_6$.

At 20 °C, the circular dichroism (CD) spectra of **1** in toluene in the presence of (*R*)- or (*S*)-**2** displayed mirror-symmetric bisignate induced circular dichroism (ICD) signals with the positive and negative maximum signals at 427 and 431 nm, respectively, and an intercept at *x*-axis (429.5 nm), which well matched the maximum in the UV/Vis spectrum (431.5 nm) (Figure 3). Interestingly, both the intensity and profiles were

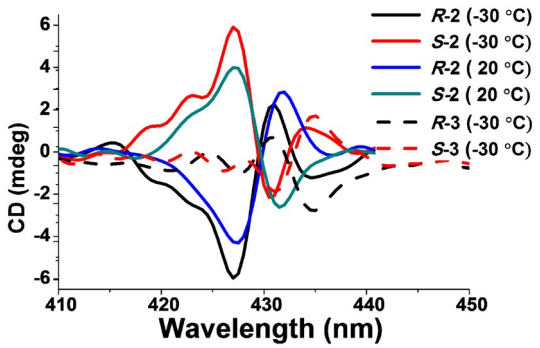

Figure 3. ICD spectra of **1** (45 μM) in toluene in the presence of *R*- and *S*-**2** (7.5 μM) at different temperatures and *R*- and *S*-**3** (7.5 μM) at −30 °C.

temperature-sensitive. The intensity of CD increased almost twice with the temperature changing from 50 °C to −20 °C (Figure S6), while the intensity of corresponding UV/Vis spectra only increased by about 25% (Figure 3 and Figure S4). A new peak centered at 434.5 nm appeared when further cooling the solution to −30 °C, and this peak was strengthened by continuously cooling the solution (Figure 3 and Figure S6) without significant change in the UV/Vis spectra (Figure S4). The solution of **1** in toluene in the presence of (*R*)- or (*S*)-**3** was CD-silent at room temperature (20 °C). When the solutions were cooled to −30 °C, mirror-symmetric bisignate ICD signals appeared with the positive and negative maximum at 431 and 435 nm, respectively (Figure 3). The intensity of the peaks strengthened when the temperature was further decreased (Figure S7).

The above CD results revealed temperature-related conformational preferences and transfers among supramolecular cages $(\mathbf{1})_6$·(*R* or *S*)-**2** and $(\mathbf{1})_6$·(*R* or *S*)-**3**. The existence of only one bisignate profile implied that there was only one kind of orderly through-space exciton coupling of the porphyrin chromophores in the chiral complex $(\mathbf{1})_6$·(*R* and *S*)-**2** above −20 °C. This could be attributed to the fast change of the twisting conformations of the biphenyl backbones (Figure 1 inset), which finally made complexes $(\mathbf{1})_6$·(*R* or *S*)-**2** C_{3v}-symtrical without regard to the pyridyl chirality and the heterocyclic cores of hexamers $(\mathbf{1})_6$ (Figure 1, State I). Therefore, the spatial orientation of the porphyrins were only affected by the chirality of the pyridine units, making all the porphyrin units to exist in the same spatial arrangement in complex $(\mathbf{1})_6$·(*R* or *S*)-**2**. When the two dominating conformations of the 1,3,5-triphenylbenzene backbone (P and M) became distinguishable at low temperatures (≤ −30 °C), complex $(\mathbf{1})_6$·(*R* or *S*)-**2** was C_3-symtrical. Besides the chirality of the pyridine units, the spatial orientation of the porphyrin units were dependent on the conformations of the 1,3,5-triphenylbenzene backbone (P and M). Therefore, porphyrins A were forced to move upward in complexes $(\mathbf{1})_6$·*R*-(M)-**2** (Figure 1, State II), giving rise to negative ICD signals centered at 434.5 nm (Figure 3). Reverse changes occurred in complex $(\mathbf{1})_6$·*S*-(P)-**2**. The ICD intensity at 434.5 nm exhibited a linear correlation with temperature (Figure S8), from which the phase transition from State I to State II was estimated to occur at −23 °C. The two states should co-exist at elevated temperature. At reduced temperature, the conformational excess, that is, State II over State I, was enhanced to generate stronger ICD signals centered at 434.5 nm (Figure S6). Considering that the phase transition started at about −23 °C (Figure S8) and completed at about −70 °C (Figure 2), the degree of the phase transition at different temperatures was estimated on the basis of the nearly linear correlation between the transition and temperature (Figure S9). It showed that the phase transition was completed by only 14% at −30 °C and by 59% at −50 °C. The plot also displayed that the degree of the phase transition increased about 20% with every 10 °C decrease in temperature. In complex $(\mathbf{1})_6$·(*R* or *S*)-**3**, the orientations of the porphyrin units were not affected by the chirality of the pyridine-connected moieties at State I because of the higher flexibility of the longer chains of **3**. At State II, porphyrins A moved upward because of the P conformation of the 1,3,5-triphenylbenzene backbone in complex $(\mathbf{1})_6$·*R*-(M)-**3**, giving rise to Cotton effects (Figure 3). This kind of conformational chirality excess was enhanced when the temperature was decreased (Figure S7).

The conformation of the 1,3,5-triphenylbenzene backbone had a pivotal impact on the A_6B-typed supramolecular cages. The rotation energy barrier from P to M of the backbone was only about 2.7 kcal mol^{-1}, as revealed by B3LYP/6-311++G(d,p) calculations (Figures S10–S11). Therefore, the conformations of the backbone switched freely at high temperatures (Figure 1, inset), making the supramolecular cages $(\mathbf{1})_6$·**2** or **3** to possess an apparent C_{3v}-symmetry (Figure 1, State I). However, the adjacent porphyrin units should orient alternately in complex $(\mathbf{1})_6$·*R*-(M or P)-**2** once the two conformations of the backbone (P and M) were distinguishable, as indicated by the molecular simulations (Figure 4 and Figure S12). The whole models of complexes $(\mathbf{1})_6$·*R*-(M)-**2** and $(\mathbf{1})_6$·*R*-(P)-**2** were optimized to reveal the differences of the binding sequences between the pyridine and zinc porphyrin units and the configurations of the hexadentate side chains (Figure S14). Keeping the conformations of hexamers $(\mathbf{1})_6$ constant in complexes $(\mathbf{1})_6$·*R*-(M)-**2** and $(\mathbf{1})_6$·*R*-(P)-**2**, the conformations of *R*-(M)-**2** and *R*-(P)-**2** were further optimized by Gaussian and molecular mechanics, respectively, which gave rise to similar results, indicating the high rationality of the molecular models (Figures S15 and S16). The energies of *R*-(M)-**2** and *R*-(P)-**2** were estimated by B3LYP/6-31G++(d,p) calculations, and the results indicated that complex $(\mathbf{1})_6$·*R*-(M)-**2** was energetically favored over $(\mathbf{1})_6$·*R*-(P)-**2** (Table S2). These results further supported the temperature-responsiveness of A_6B-typed supramolecular cages $(\mathbf{1})_6$·(*R* or *S*)-**2** and $(\mathbf{1})_6$·(*R* or *S*)-**3**. The low rotational energy barrier of the backbone brought about a free conformational change be-

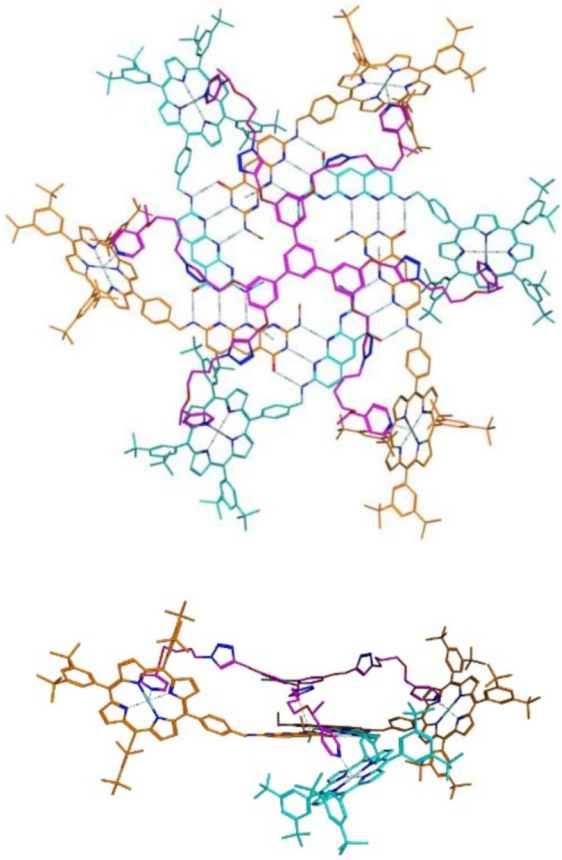

Figure 4. Molecular model of the energetically favorable complex $(\mathbf{1})_6$·*R*-(M)-**2**. Top: front view; bottom: side view (only half of the model is shown for clarity).

tween P and M at elevated temperatures, resulting in the apparent C_{3v}-symmetry of the complexes and making the spatial arrangements of the porphyrin units only being affected by the chirality of the pyridine-connected moieties (Figure 1, State I). When the two conformations (P and M) of the backbone became distinguishable at low temperatures, the conformational bias was transferred to the chains of hexadentates and then to porphyrins of hexamers. The low rotational energy barriers of the 1,3,5-triphenylbenzene backbone were thus amplified in the whole complexes. The conformational preferences of the backbones depended on the energy bias of the whole complexes. In this context, the conformational preferences of the backbones resulted in conformational chirality of the porphyrin units, which was highly temperature-dependent (Figure 1, State II).

In conclusion, temperature-dependent conformational chirality was observed in two A_6B-typed supramolecular cages, which were assembled from achiral hydrogen-bonded C_6-symmetric zinc porphyrin hexamer $(\mathbf{1})_6$ and chiral C_3-symmetric pyridine-derived hexadentates **2** and **3** by multivalent interactions. The helical conformational chirality of 1,3,5-triphenylbenzene was induced by the local chiral centers near pyridyls and confined at low temperature, which was further transferred to the whole complex.[24] The low-energy-barrier conformational preferences of the 1,3,5-triphenylbenzene backbone led to the symmetric switching of the supramolecular cages from pseudo-C_{3v} to C_3 following the decrease in temperature. The conformational preferences were transferred and amplified in the whole supramolecular entities, revealing the temperature dependence of the conformational chirality bias. The principle of the transfer and amplification of the conformational preference might be applied as a new strategy for the development of smart materials with high sensitivities and long lifetime.

Acknowledgements

We thank the National Natural Science Foundation (91227108, 21172249) and Ministry of Science and Technology of China (2013CB834501) for financial support.

Keywords: chiral transfer · conformational chirality · conformational preference · supramolecular cages · temperature-responsive

[1] a) J. Zhuang, M. R. Gordon, J. Ventura, L. Li, S. Thayumanavan, *Chem. Soc. Rev.* **2013**, *42*, 7421 – 7435; b) C. Wang, Z. Wang, X. Zhang, *Acc. Chem. Res.* **2012**, *45*, 608 – 618; c) Z. Ge, S. Liu, *Chem. Soc. Rev.* **2013**, *42*, 7289 – 7325.

[2] a) E. M. Bachelder, T. T. Beaudette, K. E. Broaders, J. Dashe, J. M. J. Frechet, *J. Am. Chem. Soc.* **2008**, *130*, 10494 – 10495; b) G. Yu, X. Zhou, Z. Zhang, C. Han, Z. Mao, C. Gao, F. Huang, *J. Am. Chem. Soc.* **2012**, *134*, 19489 – 19497; c) S. Dong, Y. Luo, X. Yan, B. Zheng, X. Ding, Y. Yu, Z. Ma, Q. Zhao, F. Huang, *Angew. Chem. Int. Ed.* **2011**, *50*, 1905 – 1909; *Angew. Chem.* **2011**, *123*, 1945 – 1949.

[3] a) R. H. Lambeth, S. Ramakrishnan, R. Mueller, J. P. Poziemski, G. S. Miguel, L. J. Markoski, C. F. Zukoski, J. S. Moore, *Langmuir* **2006**, *22*, 6352 – 6360; b) J. M. Fuller, K. R. Raghupathi, R. R. Ramireddy, A. V. Subrahmanyam, V. Yesilyurt, S. Thayumanavan, *J. Am. Chem. Soc.* **2013**, *135*, 8947 – 8954; c) X. Yan, D. Xu, X. Chi, J. Chen, S. Dong, X. Ding, Y. Yu, F. Huang, *Adv. Mater.* **2012**, *24*, 362 – 369.

[4] a) X. Wang, G. Liu, J. Hu, G. Zhang, S. Liu, *Angew. Chem. Int. Ed.* **2014**, *53*, 3138 – 3142; *Angew. Chem.* **2014**, *126*, 3202 – 3206; b) C. Wang, Q. Chen, H. Xu, Z. Wang, X. Zhang, *Adv. Mater.* **2010**, *22*, 2553 – 2555.

[5] a) J. C. Eloi, D. A. Rider, G. Cambridge, G. R. Whittell, M. A. Winnik, I. Manners, *J. Am. Chem. Soc.* **2011**, *133*, 8903 – 8913; b) C. J. Bruns, M. Frasconi, J. Iehl, K. J. Hartlieb, S. T. Schneebeli, C. Cheng, S. I. Stupp, J. F. Stoddart, *J. Am. Chem. Soc.* **2014**, *136*, 4714 – 4723; c) K.-D. Zhang, T.-Y. Zhou, X. Zhao, X.-K. Jiang, Z.-T. Li, *Langmuir* **2012**, *28*, 14839 – 14844.

[6] C. Degen, P. A. May, J. S. Moore, S. R. White, N. R. Sottos, *Macromolecules* **2013**, *46*, 8917 – 8921.

[7] J. H. Schenkel, A. Samanta, B. J. Ravoo, *Adv. Mater.* **2014**, *26*, 1076 – 1080.

[8] W. Cao, X. Zhang, X. Miao, Z. Yang, H. Xu, *Angew. Chem. Int. Ed.* **2013**, *52*, 6233 – 6237; *Angew. Chem.* **2013**, *125*, 6353 – 6357.

[9] a) C. Park, H. Kim, S. Kim, C. Kim, *J. Am. Chem. Soc.* **2009**, *131*, 16614 – 16615; b) S. U. Hettiarachchi, B. Prasai, R. L. McCarley, *J. Am. Chem. Soc.* **2014**, *136*, 7575 – 7578.

[10] a) X. Yan, Z. Li, P. Wei, F. Huang, *Org. Lett.* **2013**, *15*, 534 – 537; b) Q. Yan, R. Zhou, C. Fu, H. Zhang, Y. Yin, J. Yuan, *Angew. Chem. Int. Ed.* **2011**, *50*, 4923 – 4927; *Angew. Chem.* **2011**, *123*, 5025 – 5029; c) Z.-G. Tao, X. Zhao, X.-K. Jiang, Z.-T. Li, *Tetrahedron Lett.* **2012**, *53*, 1840 – 1842; d) S.-G. Chen, Y. Ruan, J. D. Brown, J. Gallucci, V. Maslak, C. M. Hadad, J. D. Badjic, *J. Am. Chem. Soc.* **2013**, *135*, 14964 – 14967; e) X. Ji, Y. Yao, J. Li, X. Yan, F. Huang, *J. Am. Chem. Soc.* **2013**, *135*, 74 – 77.

[11] a) R. L. McCarley, J. C. Forsythe, M. Loew, M. F. Mendoza, N. M. Hollabaugh, J. E. Winter, *Langmuir* **2013**, *29*, 13991 – 13995; b) B. Yan, J. C. Boyer, D. Habault, N. R. Branda, Y. Zhao, *J. Am. Chem. Soc.* **2012**, *134*, 16558 – 16561.

[12] a) J. Madsen, I. Canton, N. J. Warren, E. Themistou, A. Blanazs, B. Ustbas, X. Tian, R. Pearson, G. Battaglia, A. L. Lewis, S. P. Armes, *J. Am. Chem.*

Soc. **2013**, *135*, 14863 – 14870; b) C. Pietsch, R. Hoogenboom, U. S. Schubert, *Angew. Chem. Int. Ed.* **2009**, *48*, 5653 – 5656; *Angew. Chem.* **2009**, *121*, 5763 – 5766.
[13] a) A. Blanazs, R. Verber, O. O. Mykhaylyk, A. J. Ryan, J. Z. Heath, C. W. I. Douglas, S. P. Armes, *J. Am. Chem. Soc.* **2012**, *134*, 9741 – 9748; b) K. A. Mosiewicz, L. Kolb, A. J. van der Vlies, M. M. Martino, P. S. Lienemann, J. A. Hubbell, M. Ehrbar, M. P. Lutolf, *Nat. Mater.* **2013**, *12*, 1072 – 1078.
[14] a) C. Park, K. Lee, C. Kim, *Angew. Chem. Int. Ed.* **2009**, *48*, 1275 – 1278; *Angew. Chem.* **2009**, *121*, 1301 – 1304; b) E. R. Gillies, T. B. Jonsson, J. M. J. Frechet, *J. Am. Chem. Soc.* **2004**, *126*, 11936 – 11943.
[15] a) C. Kim, S. S. Agasti, Z. Zhu, L. Isaacs, V. M. Rotello, *Nat. Chem.* **2010**, *2*, 962 – 966; b) S. Himmelein, V. Lewe, M. C. A. Stuart, B. J. Ravoo, *Chem. Sci.* **2014**, *5*, 1054 – 1058.
[16] a) P. Kuad, A. Miyawaki, Y. Takashima, H. Yamaguchi, A. Harada, *J. Am. Chem. Soc.* **2007**, *129*, 12630 – 12631; b) S. K. M. Nalluri, B. J. Ravoo, *Angew. Chem. Int. Ed.* **2010**, *49*, 5371 – 5374; *Angew. Chem.* **2010**, *122*, 5499 – 5502.
[17] a) A. Laganowsky, E. Reading, T. M. Allison, M. B. Ulmschneider, M. T. Degiacomi, A. J. Baldwin, C. V. Robinson, *Nature* **2014**, *510*, 172 – 175; b) Y. Chang, R. Bruni, B. Kloss, Z. Assur, E. Kloppmann, B. Rost, W. A. Hendrickson, Q. Liu, *Science* **2014**, *344*, 1131 – 1135.
[18] J. R. Kramer, T. J. Deming, *J. Am. Chem. Soc.* **2012**, *134*, 4112 – 4115.
[19] a) S. V. Kolotuchin, S. C. Zimmerman, *J. Am. Chem. Soc.* **1998**, *120*, 9092 – 9093; b) Y. Ma, S. V. Kolotuchin, S. C. Zimmerman, *J. Am. Chem. Soc.* **2002**, *124*, 13757 – 13769.
[20] S.-G. Chen, Y.-C. Fu, G.-T. Wang, G.-Y. Li, Y. Ma, X.-K. Jiang, Z.-T. Li, *Tetrahedron* **2010**, *66*, 4057 – 4062.
[21] S.-G. Chen, Y. Yu, X. Zhao, Y. Ma, X.-K. Jiang, Z.-T. Li, *J. Am. Chem. Soc.* **2011**, *133*, 11124 – 11127.
[22] K. Hirose in *Analytical Methods in Supramolecular Chemistry* (Eds.: C. Schalley), Wiley-VCH, Weinheim, **2007**, pp. 17 – 54.
[23] A. Satake, Y. Kobuke, *Tetrahedron* **2005**, *61*, 13 – 41.
[24] M. Liu, L. Zhang, T. Wang, *Chem. Rev.* **2015**, *115*, 7304 – 7397.

Manuscript received: October 8, 2015
Revised: November 11, 2015
Final Article published: November 25, 2015